

# Concentration and Temperature Dependence of Laurdan Fluorescence in Glycerol

K. A. Kozyra<sup>a</sup>, J. R. Heldt<sup>a</sup>, J. Heldt<sup>a,b</sup>, M. Engelke<sup>c</sup>, and H. A. Diehl<sup>c</sup>

<sup>a</sup> Institute of Experimental Physics, University of Gdansk, ul. Wita Stwosza 57, Gdansk, Poland

<sup>b</sup> Institute of Physics, Pomeranian Pedagogical Academy, ul. Arciszewskiego 22B, 76-200 Slupsk, Poland

<sup>c</sup> Biophysics Group, Fachbereich 1 (Physics), Bremen University, D-28334 Bremen, Germany

Reprint requests to Dr. J. H.; Fax: +4858341-31-75; E-mail: fizjh@univ.gda.pl

Z. Naturforsch. **58a**, 581 – 588 (2003); received July 23, 2003

Steady-state and time-resolved fluorescence measurements have been performed on Laurdan, dissolved in viscous glycerol, as functions of temperature and concentration. The results indicate spectral heterogeneity of the Laurdan solution. The fluorescence decay time distribution is attributed to radiative deexcitation of spatial conformational forms of locally excited (LE) and charge transfer (CT) states, the  $S_1(\text{CT})_{\text{EQ}}$  state being in thermodynamic and vibrational equilibrium.

The lifetimes and contributions of the different fluorescence modes depend on concentration and temperature. The excitation and emission spectra show discontinuous changes with increase of the Laurdan concentration. We suppose that the observed changes are caused by the formation of Laurdan micelle aggregates.

**Key words:** Laurdan; Locally Excited and Charge Transfer States; Fluorescence Decay Time.

## 1. Introduction

Conjugated molecules which possess electron yielding and electron-withdrawing functional groups show a large change of the dipole moment on an electronic jump from the ground state [1–3]. Therefore the luminescence properties of such molecules are very sensitive to the polarity of the solvent, and the molecules are suitable probes to study the polarity of the surrounding environment. Laurdan, 6-dodecanoyl-2-dimethylaminonaphthalene (Fig. 1), belongs to this type of molecules, being used as a luminescent probe in studies of the physical and chemical properties of solvents, surfaces, membranes, cells and large biological molecules [4–10]. Due to the aliphatic tail of 12 carbons, Laurdan is supposed to anchor in the membrane and to be extremely sensitive to lipid packing, particularly at gel to liquid-crystalline membrane phase transitions. It is known that such fluorophores exhibit dual fluorescence, *i. e.* emit fluorescence from both a locally excited state,  $S_1(\text{LE})$ , and a charge transfer state,  $S_1(\text{CT})$  [11]. The ratio of the intensities of the two bands depends on the microenvironment and in many cases on the excitation wavelength, particularly on the solvent polarity and its ability to form an intermolecular complex with the solvent molecules. An

inclusion of the guest is accompanied by a decrease in the intensity of the CT emission [1, 12].

The Laurdan solution is spectrally an inhomogeneous system. As was shown in our previous work [13, 14], in the ground and excited states Laurdan dissolved in glycerol presents simultaneously a set of various conformational forms. The spatial conformational components which possess different twisting angles are the thermally distributed LE and CT states of the Laurdan molecules.

This encouraged us to extend our recent studies on the red-edge effect of the Laurdan fluorescence spectrum in glycerol [13] and to perform scrupulous measurements of the concentration and temperature dependence of the excitation and fluorescence spectra and fluorescence decay times. Results of such measurements are very important for a correct determination of different environmental factors affecting the fluorescence of soluted Laurdan. The reported results have been obtained for Laurdan dissolved in glycerol which forms a rigid matrix at low temperature (210 K), but has also relatively small viscosity at 380 K. This change of the solutions viscosity allows to determine the influence of the twisted intramolecular charge transfer on the photophysical and luminescent parameters of Laurdan.

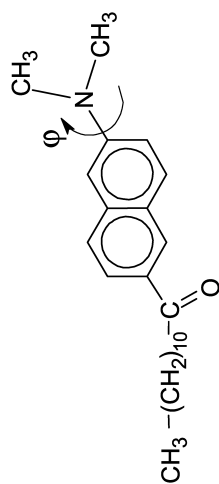
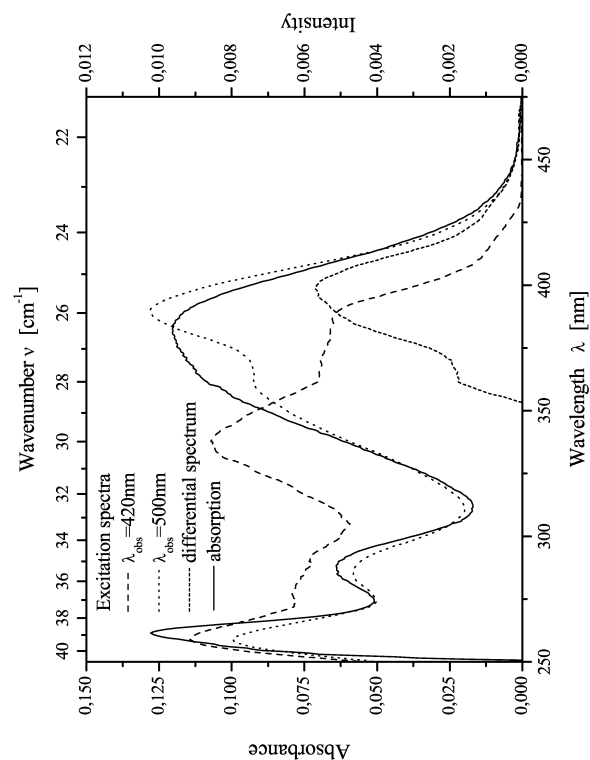


Fig. 1. Chemical structure of Laurdan.

Fig. 2. Absorption and excitation spectra of Laurdan in glycerol at room temperature.

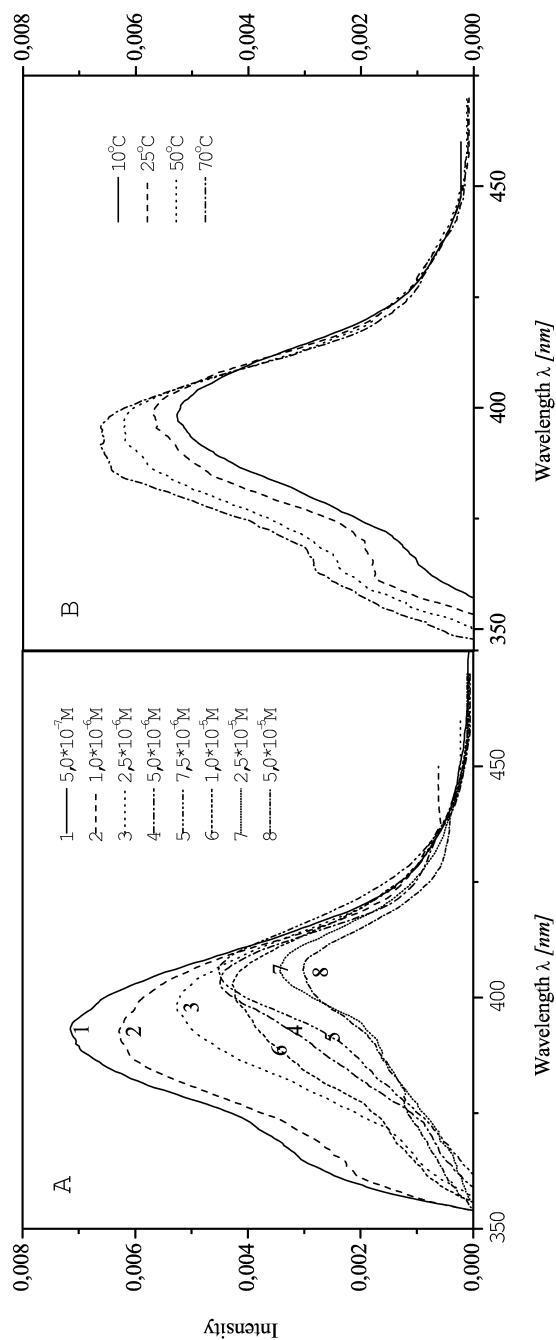


Fig. 3. Differential excitation spectra of Laurdan in glycerol as a function of dye concentration (A) and temperature (B).

We mention an alternative aspect but do not evaluate it in this paper: molecules with an aliphatic tail can form micelles. The fluorescence of such a molecule as part of a micelle may differ from that of free fluorophores, particularly when these molecules can transform into twisted intramolecular charge transfer isomers.

## 2. Experimental

Laurdan was purchased from Molecular Probes (Eugene, Oregon). The solvents glycerol and DMF (*N,N*-Dimethylformamide) were of spectroscopic grade and were obtained from Aldrich Chemical Co., Inc. After confirming the absence of absorbing and fluorescent impurities the solvent was used without further purification. Laurdan at different concentrations was dissolved in glycerol from a  $5 \times 10^{-3}$  M stock solution in DMF.

The absorption spectra were measured on a Shimadzu UV-2401PC spectrophotometer. The excitation and fluorescence spectra of the compound were obtained using a Perkin Elmer LS50 luminescence spectrofluorometer equipped with a thermostatted cuvette holder (Julabo Labortechnik, Seelbach, Germany). The measurements were carried out using  $1 \text{ cm}^2$  quartz cuvettes. The excitation spectrum was observed at 420 and 500 nm, which are the respective emission maxima in the corresponding steady state emission spectrum. The emission spectra were obtained at an excitation wavelength of 350 nm. The slit width for excitation and emission was 2.5 nm.

The fluorescence lifetime measurements were carried out using a nanosecond single photon counting apparatus. The excitation wavelength used was 403 nm. The lifetime measurements were performed at room temperature (283 K). In order to eliminate the influence of anisotropy on the decay curves, a polarizer set at the magic angle was inserted between the sample and the monochromator. The decay data analysis was performed by a reconvolution method using a non-linear least squares-fitting program. The accuracy of fit was estimated by  $\chi^2$  and standard deviation data.

## 3. Results and Discussion

### 3.1. Absorption and Excitation Spectra

The absorption and excitation spectra of Laurdan in glycerol are presented in Figure 2. The excitation and

absorption spectra are not superimposable. This difference is either caused by the presence of several species or by a single species which exists in different forms in the ground state (aggregates, micelle complexes, tautomeric forms, etc.).

The differences between the absorption and excitation spectra of Laurdan show the existence of excited molecules in different space conformations. In polar glycerol the long wavelength excitation band of Laurdan is composed of at least two bands, centred at about 340 and 390 nm. The excitation band at 390 nm is considerably more effective for emission at 500 nm. This band has been interpreted to be due to the absorption by Laurdan molecules stabilized in a ground-state L  $\alpha$  conformation by surrounding dipoles [5].

Because of the difference between these two excitation spectra we calculated “differential excitation” spectra, which give some information about the conformation of Laurdan molecules in the ground state  $S_0(\text{CT})$  beside the molecules in the  $S_0(\text{LE})$  state. The differential spectra were obtained by a mathematical operation, *e.g.* deduction from normalized  $I_{\text{exc}}(500)$  and  $I_{\text{exc}}(420)$  spectra in the region of the long wavelength absorption band. These spectra possess a maximum at 390 nm. The intensity of the differential spectrum band at 390 nm increases with temperature (Fig. 3B) and decreases with dye concentration (Fig. 3A). This dependence is understandable if we assume that the absorption of the conformational form characterized by the  $S_1(\text{CT})$  state leads to the emission band at 500 nm. With an increase of the Laurdan concentration, a decrease of free molecules in the  $S_1(\text{CT})$  state is observed. This is due to micelle-formation of Laurdan, in which the twisting angle  $\varphi$  of the mutual orientation of the  $-\text{N}(\text{CH}_3)_2$  group with respect to the plane of the naphthalene moiety is diminished. When the temperature of the solution increases, the number of emitting molecules from  $S_1(\text{CT})$  increases, because the decomposition of the aggregates increases.

### 3.2. Emission Spectra

Figure 4 shows the Laurdan fluorescence spectra in the concentration range from  $5 \times 10^{-7}$  M to  $5 \times 10^{-5}$  M measured at various temperatures: 10 °C, 25 °C, 50 °C and 70 °C. The spectra were obtained at the excitation wavelength  $\lambda_{\text{exc}} = 350$  nm. The Laurdan fluorescence in glycerol shows both, temperature and concentration dependence: for high temperatures (70 °C) the Laurdan fluorescence is mainly observed at

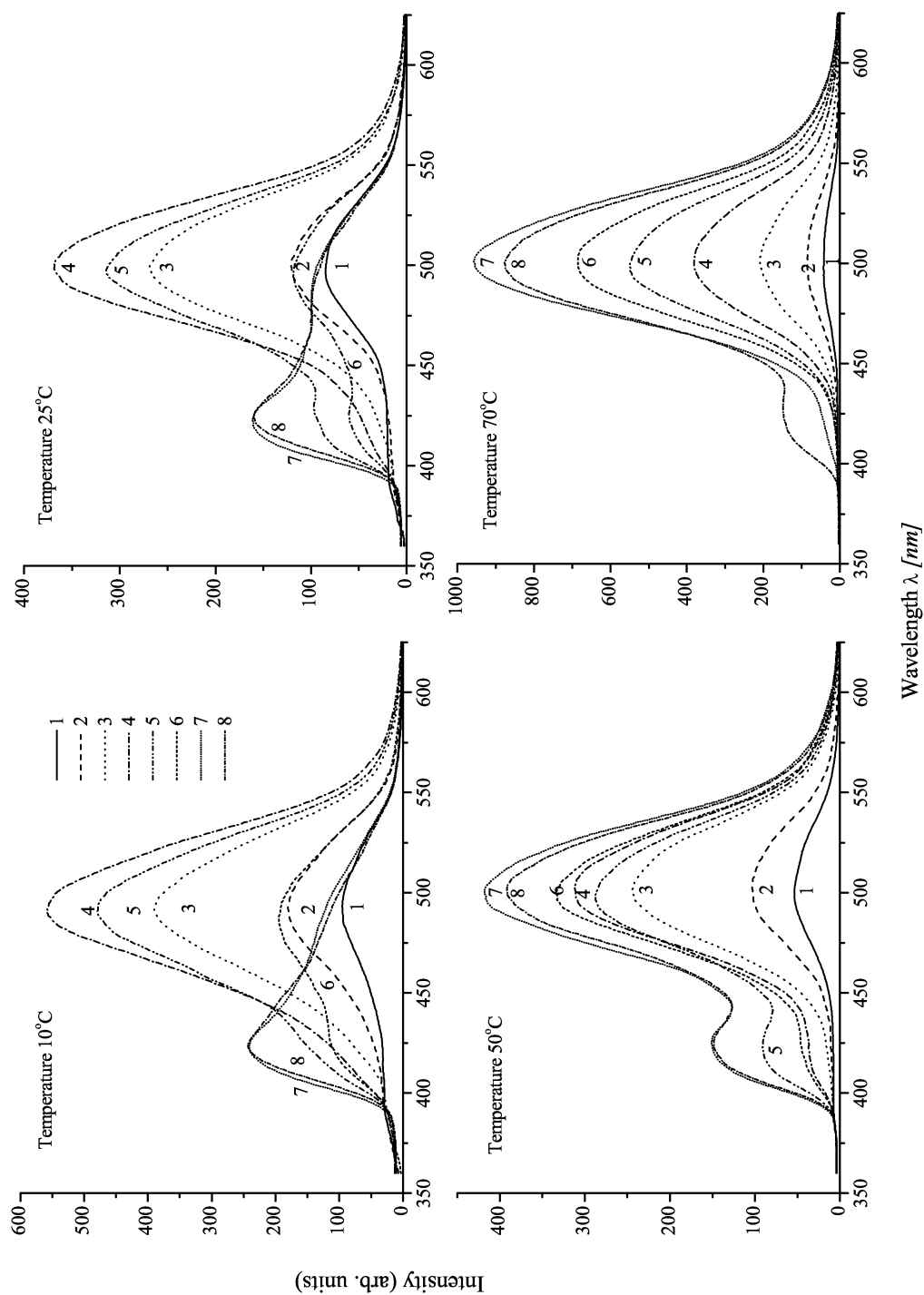


Fig. 4. Emission spectra of Laurdan as a function of the dye concentration at different temperatures. The emission spectra were excited at 350 nm. Laurdan concentrations: **1** –  $5 \times 10^{-7}$ M, **2** –  $1 \times 10^{-6}$ M, **3** –  $2.5 \times 10^{-6}$ M, **4** –  $5 \times 10^{-6}$ M, **5** –  $7.5 \times 10^{-6}$ M, **6** –  $1 \times 10^{-5}$ M, **7** –  $2.5 \times 10^{-5}$ M, **8** –  $5 \times 10^{-5}$ M.

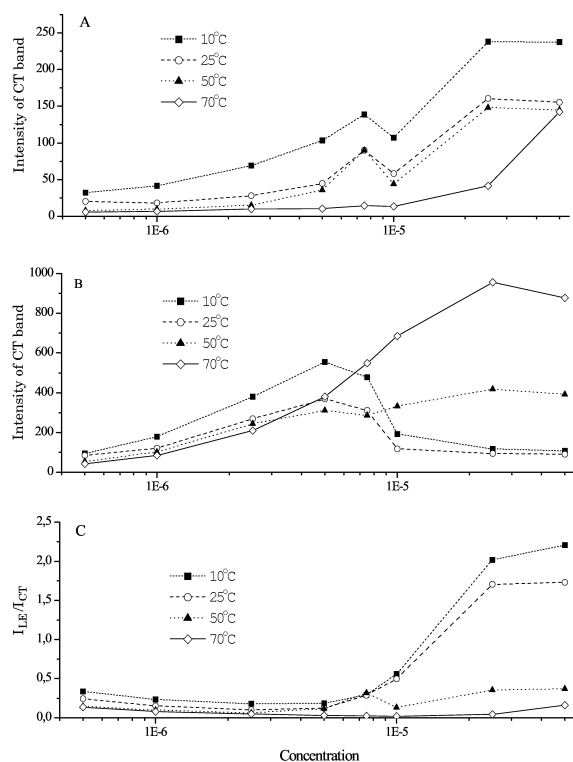


Fig. 5. A) Intensity of the LE fluorescence band as function of concentration. B) Intensity of the CT fluorescence band as function of concentration. C)  $I_{\text{LE}}/I_{\text{CT}}$  as function of concentration.

500 nm for all concentrations, whereas an increase of a second emission band at 420 nm is obtained with decreasing temperature and increasing concentration. For low concentrations of Laurdan, only one single emission band with a maximum at 500 nm is observed. For higher concentrations a second band with a maximum at 420 nm occurs. This dual fluorescence indicates the existence of two emitting species, being respectively in a locally excited  $S_1(\text{LE})$  or charge transfer  $S_1(\text{CT})$  state. The CT emission component (at 500 nm) results from transitions, starting from the  $S_1(\text{CT})$  state which is created during the lifetime of the  $S_1(\text{LE})$  excited state of Laurdan as a result of an intramolecular charge transfer phenomena between the twisted dimethylamino functional group (donor) and the naphthalene moiety (acceptor).

Figure 5 represents the dependence of the fluorescence intensity of the LE and CT bands, as well as their intensity ratio  $I_{\text{LE}}/I_{\text{CT}}$  versus the concentration of Laurdan. According to Fig. 5 an increase of Laur-

dan concentration causes an increase of LE band intensity. This behaviour does not occur at all temperatures. Generally, also the intensity of the CT band increases with concentration, but for certain concentrations it decreases (see Figs. 4 and 5). The concentration at which the intensity of the CT band decreases depends on the temperature. At  $10^{\circ}\text{C}$  this decrease occurs at  $5 \times 10^{-6}$  M. At  $70^{\circ}\text{C}$  the decrease of the CT band is observed at higher concentration, *e. g.*  $[C] = 2.5 \times 10^{-5}$  M. The intensity ratio  $I_{\text{LE}}/I_{\text{CT}}$  versus dye concentration (see Fig. 5c) shows the temperature dependence also.  $I_{\text{LE}}/I_{\text{CT}}$  increases with the concentration for the emission spectra of Laurdan in glycerol detected at 10 and  $25^{\circ}\text{C}$ , but for higher temperatures ( $50$  and  $70^{\circ}\text{C}$ ) no concentration dependence is observed.

Taking into account the structural similarities between Prodan and Laurdan, and making use of the results of theoretical studies performed for Prodan [15–19], the possibility for an existence of a CT state in Laurdan deserves special attention. In view of the quantum mechanical calculations [13], which indicate the existence of an  $S_1(\text{LE})$  and  $S_1(\text{CT})$  state and the preceding experimental observations, (the changes of the steady state fluorescence spectra of Laurdan in glycerol determined for different temperatures and concentrations), we suppose that they constitute a superposition of the emissions from two excited species, one being the precursor of the other, with a reaction rate depending on the temperature and concentration. At  $10^{\circ}\text{C}$  the contribution of the emission from the conformer with higher  $S_1(\text{LE})$  energy increases with increasing dye concentration. At higher temperatures the concentration dependence of the conformer emission is diminished. At low temperatures glycerol forms a rigid matrix in which the configuration relaxation times exceed the Laurdan lifetime of the excited  $S_1(\text{LE})$  state. For this case we observe a continuous increase of the LE emission of Laurdan with a breakdown at  $[C] = 7.5 \times 10^{-6}$  M. With increasing temperature and decreasing glycerol viscosity the condition of faster conformational changes (appearing always at  $[C] = 7.5 \times 10^{-6}$  M) result in an increase of the CT emission.

This additional concentration dependence of both emission bands requires further explanation. It is known from the literature that molecules with an aliphatic tail possess the ability to form micelles [1]. The luminescence properties of a single molecule in a micelle differ from those of a free molecule, particularly if the solute molecule besides its aliphatic tail

| Concentration<br>[M]                 | $\lambda_{\text{em}} = 420 \text{ nm}$ |             |                    | $\lambda_{\text{em}} = 500 \text{ nm}$ |                     |              |
|--------------------------------------|--|-------------|--------------------|--|---------------------|--------------|
|                                      | $\tau_i$ [ns]                          | $A_i$       |                    | $\tau_i$ [ns]                          | $A_i$               | $\chi^2$     |
| $5 \times 10^{-7}$                   | $\tau_1$                               | 0,16        | 20237 (96%)        | 0,27                                   | −4227 (23%)         | 1,127        |
|                                      | $\tau_2$                               | 1,84        | 768 (4%)           | 1,50                                   | 4522 (25%)          |              |
|                                      | $\tau_3$                               |             |                    | 3,25                                   | 9376 (52%)          |              |
| $1 \times 10^{-6}$                   | $\tau_1$                               | 0,18        | 22373 (96%)        | 0,12                                   | −6489 (33%)         | 1,145        |
|                                      | $\tau_2$                               | 1,69        | 816 (4%)           | 1,05                                   | 3773 (19%)          |              |
|                                      | $\tau_3$                               |             |                    | 3,41                                   | 9562 (48%)          |              |
| $2,5 \times 10^{-6}$                 | $\tau_1$                               | 0,20        | 21836 (91%)        | 0,11                                   | −9129 (37%)         | 1,048        |
|                                      | $\tau_2$                               | 1,49        | 2290 (9%)          | 1,02                                   | 4217 (17%)          |              |
|                                      | $\tau_3$                               |             |                    | 3,41                                   | 11540 (46%)         |              |
| $5 \times 10^{-6}$                   | $\tau_1$                               | 0,30        | 22995 (84%)        | 0,08                                   | −18576 (54%)        | 1,100        |
|                                      | $\tau_2$                               | 1,36        | 4525 (16%)         | 1,09                                   | 4516 (13%)          |              |
|                                      | $\tau_3$                               |             |                    | 3,42                                   | 11370 (33%)         |              |
| $7,5 \times 10^{-6}$                 | $\tau_1$                               | 0,49        | 13833 (76%)        | 0,09                                   | −9480 (44%)         | 1,139        |
|                                      | $\tau_2$                               | 1,59        | 4295 (24%)         | 1,22                                   | 3372 (16%)          |              |
|                                      | $\tau_3$                               |             |                    | 3,47                                   | 8781 (41%)          |              |
| <b><math>1 \times 10^{-5}</math></b> | <b><math>\tau_1</math></b>             | <b>0,29</b> | <b>11574 (62%)</b> | <b>0,77</b>                            | <b>−15597 (38%)</b> | <b>1,149</b> |
|                                      | <b><math>\tau_2</math></b>             | <b>1,04</b> | <b>6822 (38%)</b>  | <b>0,89</b>                            | <b>18254 (44%)</b>  |              |
|                                      | <b><math>\tau_3</math></b>             |             |                    | <b>3,61</b>                            | <b>7540 (18%)</b>   |              |
| $2,5 \times 10^{-5}$                 | $\tau_1$                               | 0,54        | 12786 (71%)        | 0,07                                   | −10261 (43%)        | 1,254        |
|                                      | $\tau_2$                               | 1,36        | 4930 (29%)         | 1,58                                   | 6352 (27%)          |              |
|                                      | $\tau_3$                               | 3,91        |                    |  | 7190 (30%)          |              |
| $5 \times 10^{-5}$                   | $\tau_1$                               | 0,71        | 9344 (55%)         | 0,07                                   | −11147 (47%)        | 1,310        |
|                                      | $\tau_2$                               | 1,53        | 7424 (45%)         | 1,46                                   | 5914 (25%)          |              |
|                                      | $\tau_3$                               |             |                    | 3,77                                   | 6609 (28%)          |              |

Table 1. Fluorescence decay times of Laurdan in glycerol at room temperature and their amplitudes.

$i = 1, 2, \dots, n$  for the function  $I(t) = \sum_{i=1}^n A_i \exp(-t/\tau_i)$ .

possesses the ability to form a twisted intramolecular charge transfer (TICT) isomer. Our results hint to the formation of Laurdan aggregates. Conformational changes of the Laurdan molecules within aggregates (micelles) are slow compared to those of single Laurdan molecules. Therefore, we note an increase of the LE emission with increasing dye concentration at constant temperature. This can be attributed to the micelle formation of Laurdan.

### 3.3. Excited State Lifetimes

Fluorescence decays of Laurdan in glycerol have been recorded at different concentrations at room temperature. The decay curves were recorded at  $\lambda_{\text{em}} = 420 \text{ nm}$  and  $\lambda_{\text{em}} = 500 \text{ nm}$  corresponding to the maximum intensity of the LE and CT band, respectively. The exciting wavelength of Laurdan was always  $\lambda_{\text{exc}} = 403 \text{ nm}$ . The experimental decay curves were fitted to a multiexponential function  $F(t) = \sum_{i=1}^n A_i \exp(-t/\tau_i)$ , where  $A_i$  and  $\tau_i$  are the preexponential coefficient and

decay time of the  $i$ -th component, respectively. The results of the analysis performed are collected in Table 1. Analyses of the data of Table 1 reveal that in the blue region ( $S_1(\text{LE})$  state emission at 420 nm) of the Laurdan fluorescence spectrum the decay curves are composed of two components possessing different  $\tau$  values which are sensitive to the solute concentration. Their amplitude changes with increasing Laurdan concentration. The faster decay time (described by the  $\tau_1$  value) increases with increasing Laurdan concentration, but its participation in the total emission decreases from 96% to 55%. The participation of the longer decay component, described by the  $\tau_2$  value, shows an opposite behaviour. Generally the  $\tau_2$  data decrease with increasing Laurdan concentration. An exception constitute the data obtained at about  $10^{-5} \text{ M}$  Laurdan concentration.

The fluorescence decay curves of Laurdan at 500 nm ( $S_1(\text{CT})$  state) can be satisfactorily fitted only by three temporal decay components. The shortest decay component has a negative amplitude (see Table 1). This

indicates the existence of a fast non-radiative deactivation process which leads to the depopulation of the  $S_1(\text{LE})$  state, causing an increase in the population of the emitting  $S_1(\text{CT})$  state being responsible for the CT fluorescence band at  $\lambda_{\text{max}} = 500$  nm. The analyses of the decay curves recorded at  $\lambda_{\text{em}} = 500$  nm show, that the longest lifetime decay ( $\tau_3$ ), preceded by two faster components, is only slightly sensitive to the Laurdan concentration. We suppose, taking into account the data of our former measurements [13, 14] and results of Viard *et al.* [11], that the fluorescence component decaying with  $\tau_3$  results from the emission of those Laurdan solvates which possess different spatial conformations and are in a total (vibrational and conformational) thermodynamic equilibrium. This means that special conformational forms described by the energy distribution function  $\rho_e(\varphi)$ , which depends on the twisting angle of the  $-\text{N}(\text{CH}_3)_2$  functional group with respect to the plane of the naphthalene moiety and internal oscillations of the molecule, are in equilibrium with the surrounding solution molecules. The fluorescence decay component described by the  $\tau_2$  value, similar to the respective decay component in the emission detected at  $\lambda = 420$  nm, results from the depopulation of the  $S_1(\text{CT})$  state. The differences found between the  $\tau_2$  values and pre-exponential coefficients obtained by analysing the decay curves at 420 and 500 nm, respectively, show a concentration dependence (see Table 1). Such a dependence is obvious, as has been shown in [14], in the ground state where one finds space configurations of the Laurdan molecule, which can be ascribed to the LE and CT configuration with an additional contribution from Laurdan molecules forming micelles. The latter assemble of molecules emits principally photons of the LE fluorescence band (see Fig. 4). The decay time of the two faster fluorescence modes regularly decreases with increasing concentration. The relative contribution of the CT emission to the total luminescence is strongly sensitive to the dye concentration. At a Laurdan concentration of  $[C] = 10^{-5}$  M a sudden change in lifetimes and contributions from different fluorescence modes ( $A_i$  values) is observed. This change coincides with the irregular change of the LE and CT fluorescence intensities (see Fig. 5).

The two larger fluorescence decay values are attributed to the radiative deexcitation of the locally excited (LE) state and to the charge transfer (CT) state, whereas the very short component described by  $\tau_1$  of which the sign and amplitude depend on the emission wavelength and concentration of Laurdan, is connected

to the kinetics of the donor ( $-\text{N}(\text{CH}_3)_2$  group) – acceptor (naphthalene moiety) and to dye-glycerol molecular interactions appearing in the excited state. Based on the semiempirical quantum mechanical calculations performed for Prodan, Ilich and Prendergast [17] established a plausible sequence of structural, conformational, and electronic density distribution changes in the lowest singlet excited state. According to them, the electronically excited chromophore first undergoes a structural change, which leads to a quasiseparation of the  $-\text{N}(\text{CH}_3)_2$  fragment from the naphthalene moiety. After that, as a second step, twisting of the amino group occurs. This step is a prerequisite for the formation of the CT state. The reaction

in the excited state of Laurdan can therefore be attributed to the interconversion between the excited LE and CT states, which involves a rotation of the  $-\text{N}(\text{CH}_3)_2$  group. As can be seen from the decay data, the interconversion kinetics is fast compared to the lifetime of the CT state.

In conclusion, the Laurdan molecule in glycerol exhibits  $S_1(\text{LE})$  and  $S_1(\text{CT})$  excited states. Their relative contribution to the total fluorescence emission depends on both, the viscosity of the solvent and on Laurdan aggregation.

#### 4. Conclusions

- A glycerol solution of Laurdan at any concentration represents an inhomogeneous spectroscopic medium in which multi-channel luminescence phenomena take place: a distribution of space conformational forms possessing different twisting angles, and an intramolecular charge transfer.

- The conformational forms of Laurdan emit fluorescence quanta which belong to three groups of decay times: (i) the decay time of the conformational forms with unchanged twisting angle of the  $-\text{N}(\text{CH}_3)_2$  functional group with respect to the naphthalene moiety  $\tau_1(\text{LE})$ , (ii) the Laurdan conformational form with the changed twisting angle –  $\tau_2(\text{CT})$ , and (iii) the Laurdan solvent being in thermodynamic equilibrium with the excited  $S_1(\text{CT})_{\text{EQ}}$  state – decay time  $\tau_3(\text{CT})_{\text{EQ}}$ .

- At higher concentrations, Laurdan forms micelles, a particular type of aggregates in which the twisting rotations of the  $-\text{N}(\text{CH}_3)_2$  group are damped.

- In order to distinguish the individual radiation pathways of the multi-channel luminescence of Laurdan in glycerol further experimental studies are necessary, *i. e.*, fluorescence anisotropy decay of the emis-

sion, and transient absorption measurements of the excited molecules.

#### Acknowledgements

The authors express their gratitude to Prof. Dr. Piotr Kwiek and Dr. Grzegorz Gondek for the measurements of the luminescence decay data. This work was partially supported by the research grants of the Pomeranian Pedagogical Academy at Slupsk, Project NW/6/76/03.

- [1] B. Valuer, *Molecular Fluorescence*, Wiley-Vch, Weinheim 2002.
- [2] G.E. Dobrestov, *Fluorescence Probes in Investigations of Cells, Membranes, and Lipoproteins*, Nauka, Moscow 1989 (in Russian).
- [3] A.P. Demchenko, *Luminescence and Dynamics of Protein Structure*, Naukova Dunka, Kiev 1988 (in Russian).
- [4] T. Parasassi, G. De Stasio, G. Ravagnan, R.M. Rush, and E. Gratton, *Biophys. J.* **60**, 179 (1991).
- [5] T. Parasassi, G. De Stasio, A. d'Ubaldo, and E. Gratton, *Biophys. J.* **57**, 1179 (1990).
- [6] T. Parasassi, M.D. Stefano, M. Loiero, G. Ravagnan, and E. Gratton, *Biophys. J.* **66**, 120 and 763 (1994).
- [7] H. Heerklotz, H. Binder, and G. Lantzsch, *J. Fluorescence*, **4**, 349 (1994).
- [8] R.B. McGregor and G. Weber, *Nature (London)* **319**, 273 (1986).
- [9] J.D. Bahawalkar, J. Zieba, M. Kazimierczak, P.N. Prasad, Y. Zhang, S. Ghosal, M.K. Casstevens, and R. Burzynski, *Nonlinear Opt.* **16**, 95 (1996).
- [10] G. Saroja, T. Soujanya, B. Ramachandram, and A. Samanta, *J. Fluorescence* **8**, 405 (1998).
- [11] M. Viard, J. Gallay, M. Vincent, O. Meyer, B. Robert, and M. Paternostre, *Biophys. J.* **73**, 2221 (1997).
- [12] W. Rettig and R. Lapouyade, *Fluorescence Probes Based on TICT States and other Adiabatic Reactions*, in J.R. Lakowicz (Ed.), *Topics in Fluorescence Spectroscopy*, Vol. 4 Probe Design and Chemical Sensing, Plenum Press, New York 1994, p. 109 – 149.
- [13] V.I. Tomin, M. Brozis, and J. Heldt, *Z. Naturforsch.* **58a**, 109 (2003).
- [14] M. Brozis, K.A. Kozyra, V.I. Tomin, and J. Heldt, *J. Appl. Spectr.* **69**, 412 (2002).
- [15] A.B. J. Parusel, W. Nowak, S. Grimme, and G. Köhler, *J. Phys. Chem. A* **102**, 7149 (1998).
- [16] W. Nowak, P. Adamczuk, A. Balter, and A. Sygula, *J. Mol. Struct. (Theochem)* **139**, 13 (1986).
- [17] P. Ilich and F.G. Prendergast, *J. Phys. Chem.* **93**, 4441 (1989).
- [18] Z.R. Grabowski, K. Rotkiewicz, A. Siemiarczuk, D.J. Cowley, and W. Baumann, *Nouv. J. Chim.* **3**, 443 (1979).
- [19] D. Braun and W. Rettig, *Chem. Phys.* **180**, 231 (1994).